Materials Research Proceedings **32** (2023) 173-180 https://doi.org/10.21741/9781644902615-19

Friction stir processing to improve grain refinement and superplasticity of Al-Mg-Mn-Cr alloy

Anna A. Kishchik[1,a], Ahmed O. Mosleh[2,b], Olga A. Yakovtseva[1,c], Anton D. Kotov[1,d], Anastasia V. Mikhaylovskaya[1,e*]

[1]Physical Metallurgy of Non-Ferrous Metals, National University of Science and Technology MISIS, Leninsky Prospekt, 4 build 1, 119049 Moscow, Russia

[2]Mechanical Engineering Department, Faculty of Engineering at Shoubra, Benha University

[a]kishchik.aa@misis.ru, [b]ahmed.omar@feng.bu.edu.eg, [c]yakovtsevao@mail.ru, [d]kotov@misis.ru, [e]mihaylovskaya@misis.ru

Keywords: Aluminum Alloys, Friction Stir Processing (FSP), Microstructure, Superplasticity, Grain Size

Abstract. In this study the Al-4.8Mg-1.0Mn-0.15Cr alloy was frictionally stir processed in order to enhance grain refinement effect and superplastic properties. The microstructure after friction stir processing (FSP) was analyzed using light, scanning and transmission electron microscopies. An additional cold rolling (50%) was performed after the FSP, and a comparative study in terms of microstructure and superplasticity was done between the samples processed using hot rolling and further FSP, FSP and cold rolling, and cold rolling without FSP. The superplastic properties were studied at temperatures of 450 and 500 °C with constant strain rates of 1×10^{-2} and 1×10^{-2} s^{-1}. The treatment regime including FSP and further cold rolling improved superplasticity due to fine-grained and homogeneous grain structure with a good thermal stability. At a temperature of 500°C and strain rates of 1×10^{-3} - 1×10^{-2} s^{-1} the alloy demonstrated 330-450 % elongation with a flow stress of 10-20 MPa.

Introduction

Aluminum alloys are widely used in industrial production for urban infrastructure products, due to the combination of high specific strength and corrosion resistance. The possibility of obtaining streamlined shapes is important for the automotive and aircraft industry and it is achievable with the implementation of superplastic forming. Grain boundary sliding is the key superplastic deformation mechanism that accommodated by dislocation and diffusional creep, and grain rotation [1]–[5]. Thus, for a good superplastic properties fine-grained structure and movable high angle grain boundaries are required [6]–[10]. Grain refinement improves superplasticity, strain rates and elongations increase that favor formability [11]–[13]. There are several methods for obtaining an ultrafine-grained structure (below 1 μm) in aluminum-based alloys, among the most effective are severe plastic deformation techniques [5][14][15]. A friction stir processing (FSP) is an approach of solid-state treatment to obtain a ultrafine-grained structure based on the principles of friction stir welding [16]–[19], which is relatively common in a global industry. The method is widely used to improve surface properties [20]–[22]. When processing by friction with stir, severe plastic deformation accumulates, thermal effects occur in the processing zone, which leads to the formation of fine or ultrafine recrystallized grains [17][23][24]. As the result, an increase of strength characteristics at room temperature [25] and an improvement of superplasticity are possible [26]–[30]. FSP is effective in terms of scalability and the result achieved. For a number of conventional aluminum alloys, this method improves superplasticity, including a decrease in temperature and an increase in strain rate [19][31]–[35]. It was shown in [36]–[39] that heating during FSP can lead to the growth of particles of the secondary phases, which negatively affects the mechanical properties.

Materials Research Proceedings **32** (2023) 173-180 https://doi.org/10.21741/9781644902615-19

Undesirably non-uniform distribution of secondary phase particles is noted in [40], with the formation of a depleted central zone, the mechanisms of such undesirable phenomena have not been reliably established at the moment. The authors [41] investigate the influence of the FSP parameters, the transverse speed, rotation and tilt, of the tool on the superplasticity of the conventional high-strength AA7075 alloy. At 1500 rpm, 31.5 mm/min and 2 °, under conditions of low heating in the FSP zone, a defect-free material is obtained and the alloy exhibits superplasticity at a low temperature of 400 °C. Authors of [42] investigated the influence of the processing parameters of the superplasticity of Al–4.5%Mg–0.35%Sc–0.15%Zr alloy. Comparing to a simple thermomechanical treatment, the stress reduces by 2-2.5 times and elongations increase by 2.5-7 times at low temperatures of 350-500 °C and a comparatively high strain rate of 10^{-2} s^{-1}. In recent years, there has been a growing number of scientific papers aimed to improving the application of the FSP method for obtaining semi-finished products with required characteristics of different alloys. In this work, an AA5083-type Al-Mg-Mn-Cr alloy with an increase Mn content (similar to Alnovi-U [43]) was investigated in a purpose to study the FSP influence on the grain structure and superplastic properties.

Materials and methods

For preparing the investigated alloy, technically pure elements 99.85% purity Al and 99.5% purity Mg were used. The other elements were added in the form of Al-master alloys (Al-10wt% Mn and Al-10wt% Cr). The studied alloy was casted at a temperature of 750 ± 20 °C by using a Nabertherm electric furnace. The melt was poured into a water-cooled copper mold with inner dimensions of 15×120×120 mm and casting cooling rate of ~15 K/s. After solidification, the ingot was annealed in two steps, the first step was performed at a temperature of 360 °C for 8 h and the second step was at a temperature of 420 °C for 3 h. The homogenized ingot was hot rolled from an initial thickness of 15 mm to 7 mm in a temperature of 420±20 °C.

Table 1. Chemical composition of investigated alloy (wt%).

Mg	Mn	Cr	Si	Fe	Al
4.85	1.05	0.14	0.05	0.10	Balance

A friction stir processing was performed on the surface of the rolled sheets using an automated milling machine (Bridgeport, Elmira, NY, USA). The FSP was carried out at 40 mm/min. The FSP tool was made of hot work tool steel (W302), and its design can be found in ref [44].

The FSPed samples of alloy were divided into two groups: the first group was cold rolled with a reduction of 75%, from 4 mm (plate was cut from the FSP volume) to 1 mm thickness, along the FSP direction (abbreviated by X). The second group was sliced by 1 mm in thickness sheets (abbreviated by F). Figure 1 shows a schematic diagram for these samples production. The reference treatment included hot rolling and cold rolling to 1 mm (75% reduction) without FSP (abbreviated S). Annealing in a temperature range of 400-550°C for 20 min was performed in order to analyze grain structure before the start of superplastic deformation.

The microstructure was analyzed after casting, two-step homogenization, hot rolling, FSP, cold rolling with final recrystallization annealing for 20 min in a range of 400-550°C. An Axiovert 200 MMat light microscopy (LM, Carl Zeiss Oberkochen, Germany) and a Tescan-VEGA3 scanning electron microscopy (SEM, Tescan Brno s.r.o., Kohoutovice, Czech Republic) equipped with energy dispersive spectrometr (EDS, X-MAX80, Oxford Instruments plc, Abingdon, UK) system were used. The samples were mechanically grinded using SiC papers in a range of 230 to 4000 grits, and then were polished in a solution of colloidal silica-based OPS suspension (Struers) with 20% water. The samples were anodized at a voltage of 20 V for 20 s in a 10% water solution of the H_3BO_4 saturated in the HF and then were captured using polarized light to study grain structure.

Materials Research Proceedings **32** (2023) 173-180 https://doi.org/10.21741/9781644902615-19

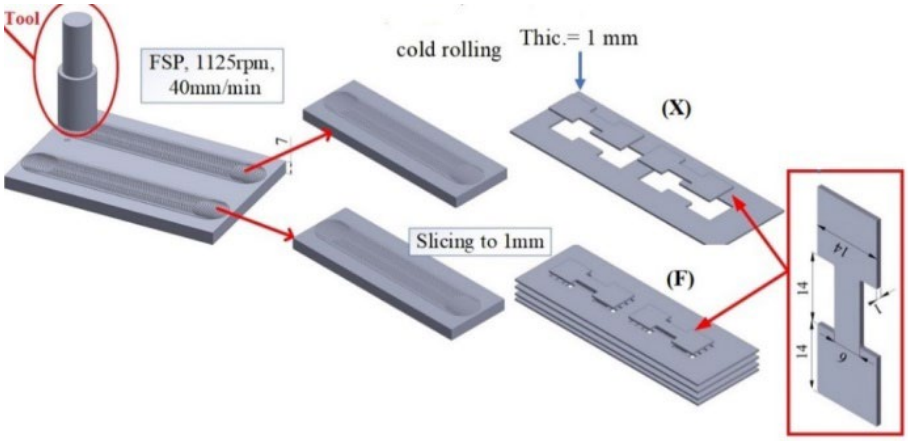

Fig. 1. Schematic diagram for sheets production methods; F is for as-FSP, and X is for FSP with subsequent cold rolling.

Results and discussion

After solidification, the dendrite liquation of Mg at the periphery of the (Al)-solid solution dendritic cells was observed (Fig. 2a). Dark areas enriched with Mg may belong to both Mg segregation and precipitates of non-equilibrium Al_3Mg_2 phase. Bright particles enriched with Mn, and also contained minor Fe and Cr, their size varied between 0.2-5 μm. After homogenization Mg distribution became homogeneous, that confirmed the elimination of the dendrite liquation and dissolution of the Mg-enriched phase (Fig.2d). Mn-bearing particles exhibited the same shape and similar size after homogenization annealing. After hot rolling the particles size decreased to 0.2-2 μm. FSP led further refinement, the size of Mn-bearing particles of solidification origin was varied in a range of 0.1-1.0 μm.

Homogenization annealing of as-cast ingot led to precipitation of elongated and equiaxed shaped dispersoids (Fig. 3a). The precipitates may belong to Al_6Mn and $Al_{18}Mg_3Cr_2$ phases, where Mn and Cr may be partially substituted by Cr, Mn, Fe [45]–[48]. The precipitates of Al_4Mn phase [49] or metastable I-phase [50]–[53] are also possible. The size of precipitates was varied in a range of 30 to 350 nm after homogenization. Hot rolling and subsequent FSP refined dispersoids to 20-140 nm. Precipitates become homogeneously distributed in matrix and their number density increased after FSP compare to hot rolled state (Fig.2c,f).. It is notable, that dispersoids demonstrated the same size after multidirectional forging with cumulative strain of $\sum e=10.5$ for alloy of a similar composition [54]. Fine Al_6Mn dispersoids help to pin grain boundaries and provide stable grain size [25][55].

The morphology of the as-cast grains was characterized by a dendritic structure (Fig. 4a). The average grain size was 150±30 μm. Before the FSP, the microstructure of the hot-rolled alloy (base metal, BM) was non-recrystallized and it was characterized by the large grains with a liner size in a range of 20-300 μm (Fig. 4b) After FSP, grain size was significantly decreased (Fig. 4c,d). The stir zone exhibited a fine-grained structure with a mean size of 4.0±0.3 μm (Fig. 4d).

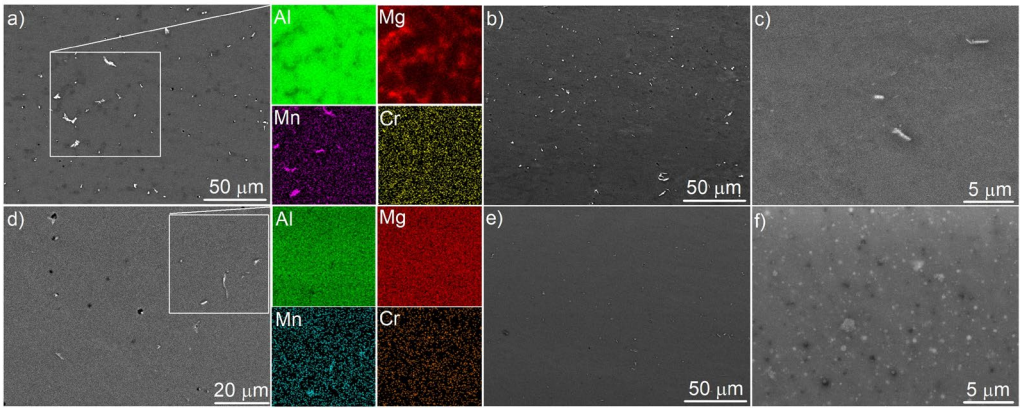

Fig. 2. The SEM micrographs with corresponding EDS maps of the as-cast alloy (a), after homogenization annealing (d), after hot rolling (b,c) and after FSP (e,f) for the Al-Mg-Mn-Cr alloy.

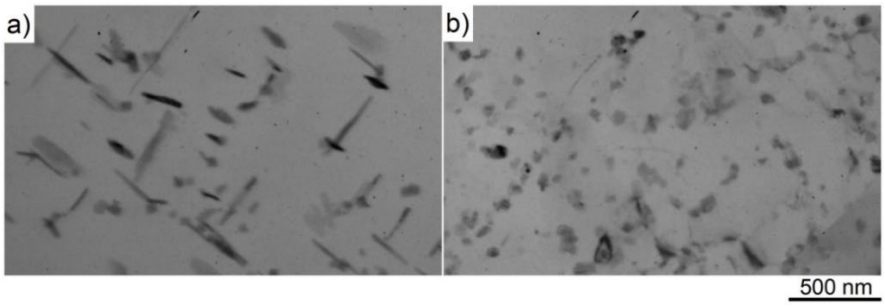

Fig.3. TEM micrographs of the alloy after homogenization (a) and FSP in a stir zone (b)

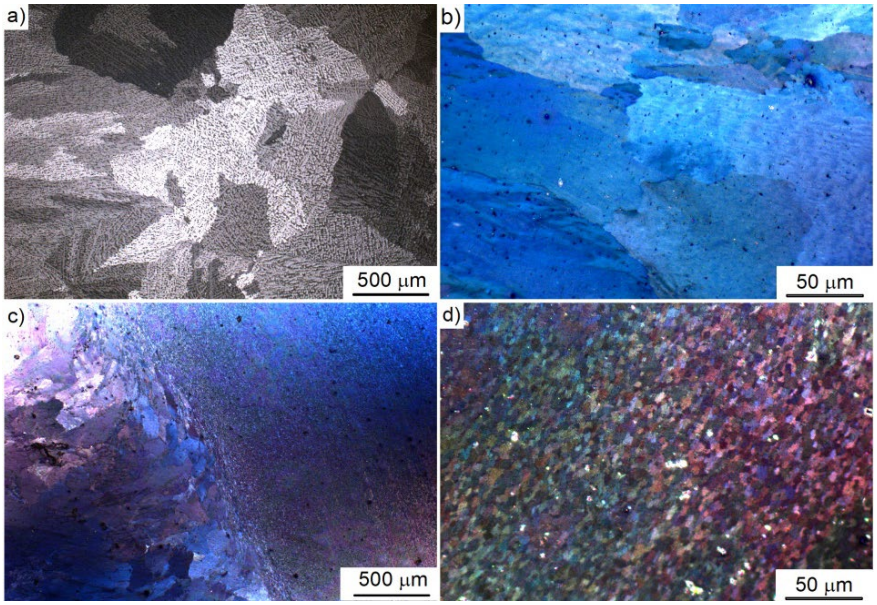

Fig. 4. The microstructures for the alloy: as-cast (a), after hot rolling (b) and after FSP (c,d).

Figure 5 shows the grain structure after annealing for 20 min for the alloys with different treatments. For FSP alloy (regime F), equiaxed grains with a mean grain size of 4.8±0.4 μm were formed at 400 °C (Fig. 5a) and with a mean grain size of 12.5±0.8 μm at 500 °C (Fig. 5c). The sheets treated by X regime with FSP and cold rolling demonstrated grain size of 7.1±0.6 μm at 400 °C (Fig. 5e) and 7.6±0.5 μm at 500 °C (Fig. 5g) and equiaxed grain structure. The alloy after a simple thermomechanical treatment included hot and cold rolling (reference regime S)

demonstrated a mean grain size of 11±1 μm after annealing at both 450 and 500 °C (Fig. 5j,k). Meanwhile, more elongated grains were formed after simple treatment 'S'. The grain aspect ratio was ~1 for F and X treatment and varied between 0.3 to 0.6 for 'S' treatment.

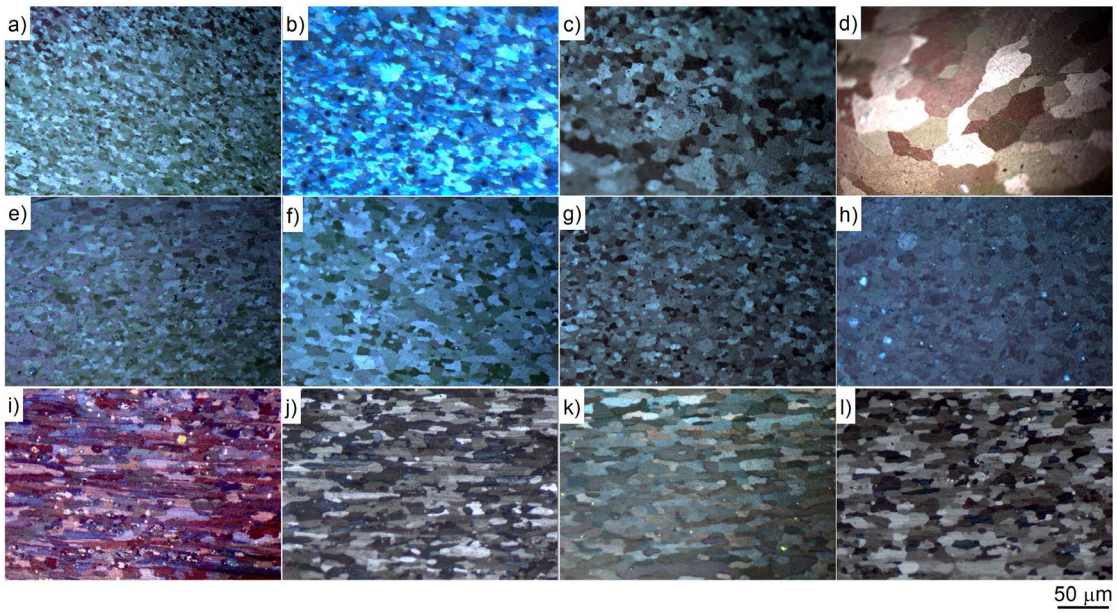

Fig. 5. The microstructure of the Al-Mg-Mn-Cr alloy after annealing at 400 °C (a,e,i); 450 °C (b,f,j), 500 °C (c,g,k) and 550 °C (d,h,l) treated by hot rolling and FSP (F regime) (a-d), hot rolling, FSP and cold rolling (X regime) (e-h), hot rolling and cold rolling (S regime) (i-l).

Figure 6a shows the stress *vs.* strain rate and strain rate sensitivity *m*-coefficient *vs.* strain rate dependences for the studied alloy after different treatment regimes, F, X, and S, at the temperatures of 450 °C and 500 °C. The curves demonstrated sigmoidal shape that is usual for superplastic materials. The maximum *m*-values were corresponded to 1×10^{-3} s^{-1} for the samples processed by the X and S regimes, and near 1×10^{-2} s^{-1} for the FSP mode, the F regime. The constant strain rate tests were perfumed at both strain rates 1×10^{-3} s^{-1} and 1×10^{-2} s^{-1} (Fig. 6b). Stress level decreased with a decrease in a strain rate and an increase in deformation temperature. The F treated and S treated alloys demonstrated small elongations of 160-250% at both strain rates studied. Regime X with FSP and cold rolling demonstrated similar values of 250% at 450° C. Higher temperature of 500°C provided 330% of elongation at 1×10^{-2} s^{-1} and 450% of elongation to failure at 1×10^{-3} s^{-1}. Small elongations of FSP treated F-type alloy is the result of weak grain size stability, meanwhile, rolling after FSP provided a stable fine-grained structure and good superplastic properties.
Thus, FSP as an intermediate processing operation provided a fine grained equiaxed structure and good superplasticity. An equiaxed grained structure and high grain size stability of the FSP treated and cold rolled samples and the resulted large elongations can be the result of a high fraction of fine dispersoids provided a high Zener drag force, uniform distribution and fine size of the solidification-originated particles.

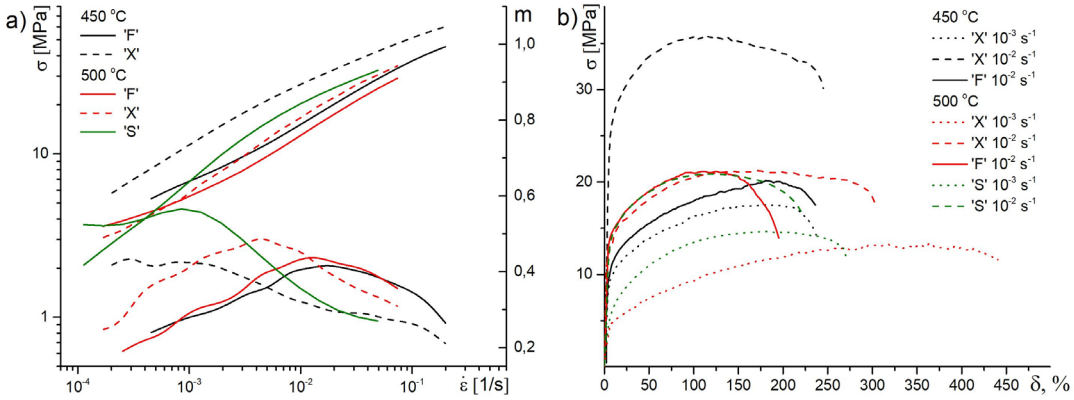

Fig. 6. Strain rate dependences of the flow stress and parameter m for a temperature of 450 °C and 500 °C (a) and dependences of the flow stress on deformation at strain rate of 1×10^{-2} s^{-1} for the investigated alloy for different technologies.

Summary

Three treatment regimes including (F) hot rolling and FSP, (X) hot rolling, FSP and cold rolling, and (S) hot rolling and cold rolling were compared for Al4.8Mg-1Mn-0.1Cr alloy.

Friction stir processing refined phases of solidification origin and dispersoids and provided an eqiaxed recrystallized fine-grained structure with a mean grain size of ~4 μm in a stir zone. Increasing an annealing temperature for the FSP-processed samples in arrange of 400-550°C led a significant grain growth from 4.8 μm to 40 μm, with abnormal grain growth at 550°C. A weak grain structure stability was a reason of low superplastic properties. A simple treatment 'S' with hot and cold rolling forms an elongated grains with a mean longitudinal size of 10.9 μm and aspect ratio of 0.6 after annealing at the same temperature range. An elongated grains of the S-treated alloy also lead a weak superplasticity. Oppositely, the treatment X including hot rolling, FSP and cold rolling provided a fine-grained equiaxed structure after annealing in a temperature range of 400-550 °C with a mean size of 7.1-8.5 μm. This treatment provide a good superplasticity at 500°C with m ~0.5 and 330-450% of elongation to failure at strain rates of 1×10^{-3} - 1×10^{-2} s^{-1}.

Acknowledgment

The study was funded by the RSF Grant # 22-79-00215.

References

[1] A.H. Chokshi, Adv. Eng. Mater. 2020, 22, 1900748. https://doi.org/10.1002/adem.201900748
[2] A.K. Basak, A. Pramanik, C. Prakash, S. Shankar, S.S. Sehgal, Mater. Today Commun. 2023, 35. https://doi.org/10.1016/j.mtcomm.2023.105830
[3] H. Masuda, T. Kanazawa, H. Tobe, E. Sato, Scr. Mater. 2018, 149, 84. https://doi.org/10.1016/j.scriptamat.2018.02.021
[4] H. Masuda, E. Sato, Acta Mater. 2020, 197, 235. https://doi.org/10.1016/j.actamat.2020.07.042
[5] T.G. Langdon, J. Mater. Sci. 2007, 42, 3388. https://doi.org/10.1007/s10853-006-1475-8
[6] E. V. Bobruk, P.D. Dolzhenko, M.Y. Murashkin, R.Z. Valiev, N.A. Enikeev, Materials (Basel). 2022, 15, 6983. https://doi.org/10.3390/ma15196983
[7] E. V. Bobruk, M.Y. Murashkin, I.A. Ramazanov, V.U. Kazykhanov, R.Z. Valiev, Materials (Basel). 2023, 16, 727. https://doi.org/10.3390/ma16020727
[8] M. Kawasaki, T.G. Langdon, Mater. Trans. 2019, 60, 1123. https://doi.org/10.2320/matertrans.MF201915
[9] R.B. Figueiredo, M. Kawasaki, T.G. Langdon, Prog. Mater. Sci. 2023, 137, 101131. https://doi.org/10.1016/j.pmatsci.2023.101131

[10] F.A. Mohamed, Adv. Eng. Mater. 2020, 22, 1900532. https://doi.org/10.1002/adem.201900532
[11] L. Bhatta, A. Pesin, A.P. Zhilyaev, P. Tandon, C. Kong, H. Yu, Metals (Basel). 2020, 10, 77. https://doi.org/10.3390/met10010077
[12] T.G. Nieh, J. Wadsworth, O.D. Sherby, O.D.S.T.G.N. J. Wadsworth, Superplasticity in Metals and Ceramics, Cambridge University Press, New York 1997. https://doi.org/10.1017/CBO9780511525230
[13] T.G. Langdon, Acta Metall. Mater. 1994, 42, 2437. https://doi.org/10.1016/0956-7151(94)90322-0
[14] K. Higashi, Mater. Sci. Technol. 2000, 16, 1320. https://doi.org/10.1179/026708300101507172
[15] T.G. Langdon, Mater. Trans. JIM 1999, 40, 716. https://doi.org/10.2320/matertrans1989.40.716
[16] V. Patel, W. Li, A. Vairis, V. Badheka, Crit. Rev. Solid State Mater. Sci. 2019, 44, 378. https://doi.org/10.1080/10408436.2018.1490251
[17] R.S. Mishra, Z.Y. Ma, Mater. Sci. Eng. R Reports 2005, 50, 1. https://doi.org/10.1016/j.mser.2005.07.001
[18] D. Lohwasser, Z. Chen, in Frict. Stir Weld., Elsevier2010, 1. https://doi.org/10.1533/9781845697716.1
[19] Z.Y. Ma, R.S. Mishra, F.C. Liu, Mater. Sci. Eng. A 2009, 505, 70. https://doi.org/10.1016/j.msea.2008.11.016
[20] K.M. Mehta, V.J. Badheka, Wear 2023, 522, 204719. https://doi.org/10.1016/j.wear.2023.204719
[21] Z. Wei, A. Kulandaivel, T. Hermanto, R. Vaira Vignesh, S. Mehrez, M. Paidar, A. Mohd Zain, V. Mohanavel, Mater. Lett. 2023, 346, 134532. https://doi.org/10.1016/j.matlet.2023.134532
[22] Shalok Bharti, N.D. Ghetiya, K.M. Patel, Phys. Met. Metallogr. 2022, 123, 1387. https://doi.org/10.1134/S0031918X21100586
[23] S. Malopheyev, S. Mironov, R. Kaibyshev, Mater. Charact. 2023, 200, 112909. https://doi.org/10.1016/j.matchar.2023.112909
[24] S. Mironov, Y.S. Sato, H. Kokawa, Acta Mater. 2008, 56, 2602. https://doi.org/10.1016/j.actamat.2008.01.040
[25] I. Vysotskii, S. Malopheyev, S. Mironov, R. Kaibyshev, Mater. Charact. 2022, 185, 111758. https://doi.org/10.1016/j.matchar.2022.111758
[26] H. Mirzadeh, Mater. Sci. Eng. A 2021, 819, 141499. https://doi.org/10.1016/j.msea.2021.141499
[27] Y.B. Sun, X.P. Chen, J. Xie, C. Wang, Y.F. An, Q. Liu, Mater. Today Commun. 2022, 33, 104217. https://doi.org/10.1016/j.mtcomm.2022.104217
[28] F. Cao, C. Xiang, S. Kong, N. Guo, H. Shang, Materials (Basel). 2023, 16, 2345. https://doi.org/10.3390/ma16062345
[29] A. Orozco-Caballero, M. Álvarez-Leal, F. Carreño, O.A. Ruano, Metals (Basel). 2022, 12, 1880. https://doi.org/10.3390/met12111880
[30] J. He, Y. Hu, Y. Sun, W. Li, G. Luo, Mater. Res. Express 2022, 9, 096509. https://doi.org/10.1088/2053-1591/ac8f20
[31] X.C. Luo, D.T. Zhang, G.H. Cao, C. Qiu, D.L. Chen, Mater. Sci. Eng. A 2019, 759, 234. https://doi.org/10.1016/j.msea.2019.05.050

[32] I. Charit, R.S. Mishra, Mater. Sci. Eng. A 2003, 359, 290. https://doi.org/10.1016/S0921-5093(03)00367-8
[33] I. Charit, R.S. Mishra, Acta Mater. 2005, 53, 4211. https://doi.org/10.1016/j.actamat.2005.05.021
[34] Z.. Ma, R.. Mishra, M.. Mahoney, Acta Mater. 2002, 50, 4419. https://doi.org/10.1016/S1359-6454(02)00278-1
[35] F.C. Liu, B.L. Xiao, K. Wang, Z.Y. Ma, Mater. Sci. Eng. A 2010, 527, 4191. https://doi.org/10.1016/j.msea.2010.03.065
[36] A. Denquin, D. Allehaux, M.H. Campagnac, G. Lapasset, Mater. Sci. Forum 2003, 426-432, 2921. https://doi.org/10.4028/www.scientific.net/MSF.426-432.2921
[37] B. Yang, J. Yan, M.A. Sutton, A.P. Reynolds, Mater. Sci. Eng. A 2004, 364, 55. https://doi.org/10.1016/S0921-5093(03)00532-X
[38] H.G. Salem, Scr. Mater. 2003, 49, 1103. https://doi.org/10.1016/j.scriptamat.2003.08.010
[39] V. V. Patel, V. Badheka, A. Kumar, Mater. Manuf. Process. 2016, 31, 1573. https://doi.org/10.1080/10426914.2015.1103868
[40] A. Smolej, D. Klobčar, B. Skaza, A. Nagode, E. Slaček, V. Dragojević, S. Smolej, Mater. Sci. Eng. A 2014, 590, 239. https://doi.org/10.1016/j.msea.2013.10.027
[41] A. Jamali, S.E. Mirsalehi, CIRP J. Manuf. Sci. Technol. 2022, 37, 55. https://doi.org/10.1016/j.cirpj.2021.12.008
[42] S. Pradeep, V. Pancholi, Metall. Mater. Trans. A 2014, 45, 6207. https://doi.org/10.1007/s11661-014-2573-x
[43] T. Kudo, A. Goto, K. Saito, in Mater. Sci. Forum, 2013, 271. https://doi.org/10.4028/www.scientific.net/MSF.735.271
[44] A.O. Mosleh, O.A. Yakovtseva, A.A. Kishchik, A.D. Kotov, E.B. Moustafa, A. V. Mikhaylovskaya, JOM 2023.
[45] O. Engler, S. Miller-Jupp, J. Alloys Compd. 2016, 689, 998. https://doi.org/10.1016/j.jallcom.2016.08.070
[46] B. Yang, M. Gao, Y. Liu, S. Pan, S. Meng, Y. Fu, R. Guan, Mater. Sci. Eng. A 2023, 872, 144952. https://doi.org/10.1016/j.msea.2023.144952
[47] S. Pan, Z. Wang, C. Li, D. Wan, X. Chen, K. Chen, Y. Li, Mater. Des. 2023, 226, 111647. https://doi.org/10.1016/j.matdes.2023.111647
[48] M. Mofarrehi, M. Javidani, X.-G. Chen, Mater. Sci. Eng. A 2022, 845, 143217. https://doi.org/10.1016/j.msea.2022.143217
[49] A.Y. Algendy, K. Liu, X.G. Chen, Mater. Charact. 2021, 181, 111487. https://doi.org/10.1016/j.matchar.2021.111487
[50] A.G. Mochugovskiy, N.Y. Tabachkova, M.E. Ghayoumabadi, V.V. Cheverikin, A.V. Mikhaylovskaya, J. Mater. Sci. Technol. 2021, 87, 196. https://doi.org/10.1016/j.jmst.2021.01.055
[51] A.G. Mochugovskiy, N.Y. Tabachkova, A.V. Mikhaylovskaya, Mater. Lett. 2021, 284, 128945. https://doi.org/10.1016/j.matlet.2020.128945
[52] A. Mochugovskiy, N. Tabachkova, A. Mikhaylovskaya, Mater. Lett. 2019, 247, 200. https://doi.org/10.1016/j.matlet.2019.03.126
[53] F. Zupanič, T. Bončina, Solid State Phenom. 2022, 327, 26. https://doi.org/10.4028/www.scientific.net/SSP.327.26
[54] A.A. Kishchik, M.S. Kishchik, A.D. Kotov, A.V. Mikhaylovskaya, Phys. Met. Metallogr. 2020, 121, 489. https://doi.org/10.1134/S0031918X20050075
[55] I. Nikulin, A. Kipelova, S. Malopheyev, R. Kaibyshev, Acta Mater. 2012, 60, 487. https://doi.org/10.1016/j.actamat.2011.10.023